

PAPER • OPEN ACCESS

Formation and optical properties of hybrid organic-inorganic MAPbI₃ perovskite films

To cite this article: T Zelenyak *et al* 2019 *IOP Conf. Ser.: Mater. Sci. Eng.* **498** 012012

View the [article online](#) for updates and enhancements.



IOP | ebooks™

Bringing you innovative digital publishing with leading voices to create your essential collection of books in STEM research.

Start exploring the collection - download the first chapter of every title for free.

Formation and optical properties of hybrid organic-inorganic MAPbI₃ perovskite films

T Zelenyak^{1*}, V Kinev¹, P Rezepov¹, O Korolik², A Mazanik², M Tivanov²,
N Doroshkevich³, A Lavysh⁴, V Gevorgyan⁶, A Tameev⁵, A Vannikov⁵,
V Turchenko^{3,6} and P Gladyshev¹

¹ State University "Dubna", Dubna, Moscow region, Russia

² Belarusian State University, Minsk, Belarus

³ Joint Institute for Nuclear Research, Dubna, Moscow region, Russia

⁴ Yanka Kupala State University of Grodno, Grodno, Belarus

⁵ Institute of Physical Chemistry and Electrochemistry. A.N Frumkin, RAS, Moscow, Russia

⁶ Russian-Armenian (Slavonic) University, Erevan, Armenia

*Corresponding author's e-mail address: tatyana.zelenyak@bk.ru

Abstract. A rapid progress in the development of solar cells based on hybrid organic-inorganic perovskites CH₃NH₃PbI₃ (MAPbI₃) is observed in recent years, and power conversion efficiency as high as 22.1 % has been reported. However, a low stability is the main drawback of these materials, which impedes their practical use for solar energy conversion. This work is devoted to the synthesis of CH₃NH₃PbI₃ films from CH₃NH₃I and PbI₂ precursors and spectroscopic investigation of their stability under high-intensity laser illumination.

1. Introduction.

The first successful attempt to prepare semiconductor organic-inorganic perovskite MAPbI₃ (MA = CH₃NH₃) for solar energy conversion has been reported in 2009 [1]. This class of semiconductors has attracted a lot of attention due to high light absorption, band gap energy close to the optimal value, sufficiently large lifetime of non-equilibrium charge carriers (up to 1 μs), possibility of solution based synthesis [2]. Solar cells based on ABX₃ perovskites have reached power conversion efficiency of 22.1 % for a short time [3].

Low-temperature wet methods (spin-coating, drop casting, dip coating, doctor blading, screen-printing, spray methods) are used most commonly to synthesize perovskite materials [4]. Solution based methods of synthesis of MAPbI₃ thin films can be divided into one- and two-stage. In the first case, the films are formed by mixing of methylammonium iodide (MAI) and lead iodide PbI₂ solutions. The two-stage approach includes deposition of PbI₂ layer at the first stage, which is followed by its transformation to MAPbI₃ by MAI intercalation. Morphology and quality of the films prepared using the one-stage method are determined mainly by the film shrinkage during the perovskite crystallization and removing of the solvent. The main problem of the two-stage method is expansion of PbI₂ film during intercalation of MAI [5].

A low stability of hybrid organic-inorganic perovskite films is known as the main impediment for their practical use in photovoltaics [4]. This makes extremely important revealing degradation



mechanisms and looking for the ways to reduce it. In this work, we analyze transformation of optical properties of $\text{CH}_3\text{NH}_3\text{PbI}_3$ films under influence of optical illumination with different power density.

2. Experimental

2.1 Film preparation

$\text{CH}_3\text{NH}_3\text{PbI}_3$ films were prepared using PbI_2 and $\text{CH}_3\text{NH}_3\text{I}$ precursors according to the previously described procedures [6-11]. All reagents were purchased from Sigma Aldrich.

One-stage method. 0.395 g of $\text{CH}_3\text{NH}_3\text{I}$ and 1.157 g of PbI_2 (99%) were dissolved in 2 ml of N,N – dimethylformamide (DMFA, $\text{C}_3\text{H}_7\text{NO}$). The obtained solution was stirred with a magnetic stirrer for 12 h at 60 °C and then spin-coated on the cleaned FTO glass substrate ($25 \times 25 \text{ mm}^2$) under normal conditions. Rotating speed was 500 RPM for the first 10 s, 2000 RPM for the second 10 s and 5000 RPM for the last 20 s. To avoid crystallization of lead iodide, the working solution was maintained at the temperature from 60 to 80 °C before deposition. The obtained films were annealed for 30 min at 100 °C on a hot plate, which resulted in formation of $\text{CH}_3\text{NH}_3\text{PbI}_3$.

Two-stage method. To obtain PbI_2 solution, 1 g of PbI_2 was dissolved in 2 ml of DMFA (purity better than 99%) and stirred at 120 °C for 1 h. The prepared solution was kept at 80 °C until its deposition. 40 μl of solution was spin-coated on FTO glass substrate (500 RPM for 10 s, 2000 RPM for 10 s, and 4000 RPM for 20 s). The obtained PbI_2 film was annealed for 15 min at 70 °C on a hot plate.

$\text{CH}_3\text{NH}_3\text{I}$ solution was prepared immediately before its use by a careful stirring of $\text{CH}_3\text{NH}_3\text{I}$ in anhydrous isopropyl alcohol (purity better than 99%, 10 mg/ml) for 15 min at room temperature.

The prepared PbI_2 film was dipped into $\text{CH}_3\text{NH}_3\text{I}$ solution for 60 s, washed with anhydrous 2-propanol to remove unreacted $\text{CH}_3\text{NH}_3\text{I}$ and finally annealed for 30 min at 80 °C on a hot plate.

Since prepared $\text{CH}_3\text{NH}_3\text{PbI}_3$ films demonstrate well-known fast degradation during ambient storage (Figure 1a), they were covered by a thin (0.15 mm) glass coverslip with a thorough sealing of the end faces with a silicone hermetic immediately after synthesis.

2.2 Characterization

X-ray diffraction analysis was performed with an Empyrean diffractometer (PANalytical, Cu $K\alpha$ emission). UV-Vis-NIR transmission spectra were measured in the 400 – 1100 nm range with an UNICO 2804 (UNICO, USA) single-beam spectrometer.

Raman and photoluminescence (PL) spectra were measured at room temperature using a Nanofinder HE confocal spectrometer (LOTIS TII, Belarus-Japan) with 532 nm DPSS laser as an excitation source. Back-scattered light without analysis of its polarization was dispersed with a spectral resolution of 2.5 cm^{-1} (0.1 nm) and detected with a cooled CCD-matrix. 50x Olympus lens (numerical aperture of 0.8) was used to focus laser beam on the surface of $\text{CH}_3\text{NH}_3\text{PbI}_3$ film. Spectral calibration was done using a built-in gas-discharge lamp providing accuracy better than 2.5 cm^{-1} (0.1 nm).

PL decay kinetics were measured in the time-correlated single photon counting mode. PDL 800-B laser with LDH-P-C-470 laser head (PicoQuant, Germany) was used providing excitation at wavelength of 467 nm with pulse duration and frequency of 73 ps and 10 MHz, respectively. Low power density in these experiments (10 W/m^2) ensured their non-destructive character. PL decay detection system included PMA-182 photodetector with TimeHarp200 device (PicoQuant, Germany) for time-correlated single photon counting measurements. The obtained kinetics were analyzed taking into account that the measured PL intensity $I(t)$ is the convolution of the instrument response function (IRF, $g(t)$) and “true” PL decay function $F(t)$:

$$I(t) = g(t) \otimes F(t) = \int_0^t g(t')F(t-t')dt' \quad (1)$$

3. Results and discussions

Our experiments have demonstrated that two-stage method is preferable to prepare $\text{CH}_3\text{NH}_3\text{PbI}_3$ films, because it provides better control of their properties and better uniformity. Therefore, the films prepared using two-stage method were chosen for investigation of optical properties.

XRD analysis at room temperature demonstrates the tetragonal crystal structure of $\text{CH}_3\text{NH}_3\text{PbI}_3$ films (Figure 1). Differential scanning calorimetry reveals a transition from tetragonal to cubic phase at 53–57 °C.

Typical absorption spectra of PbI_2 (reference) and $\text{CH}_3\text{NH}_3\text{PbI}_3$ films are presented in Figure 1b. PbI_2 films demonstrate a pronounced absorption edge at 515 nm, which corresponds to the band gap energy of 2.4 eV [13]. Transformation of PbI_2 to $\text{CH}_3\text{NH}_3\text{PbI}_3$ results in a shift of absorption edge to appr. 780 nm in agreement with [14,15]. Absorption spectra of $\text{CH}_3\text{NH}_3\text{PbI}_3$ films point to a significant light scattering related to formation of large $\text{CH}_3\text{NH}_3\text{PbI}_3$ crystals [13]. Spectra plotted in the absorbance – energy coordinates (inset in Figure. 1b) allowed determination of band gap energy of $\text{CH}_3\text{NH}_3\text{PbI}_3$ (≈ 1.50 eV), which is in a good agreement with literature data [16,17].

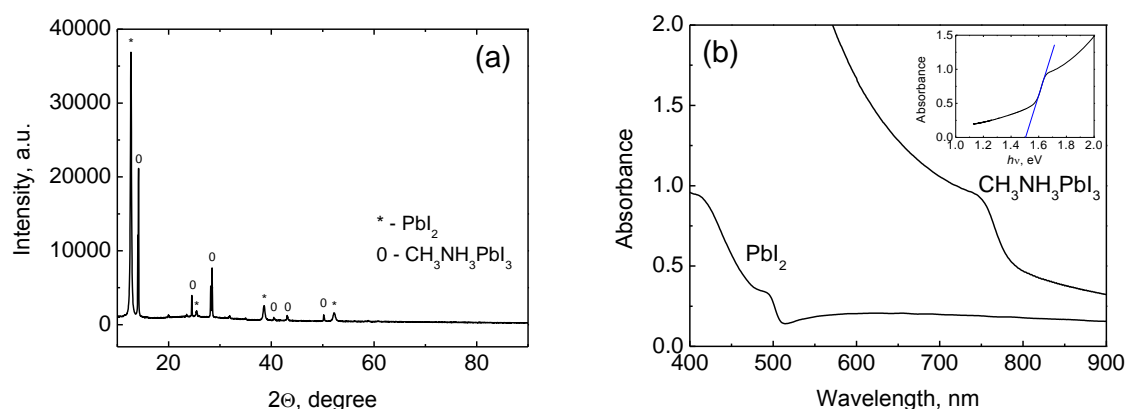


Figure 1. XRD pattern of unsealed $\text{CH}_3\text{NH}_3\text{PbI}_3$ film (a); UV-Vis-NIR absorption spectra of $\text{CH}_3\text{NH}_3\text{PbI}_3$ and PbI_2 films (b).

The prepared $\text{CH}_3\text{NH}_3\text{PbI}_3$ films reveal an intensive PL peak with maximum at appr. 0.77 μm (Figure 2a), which corresponds to interband radiative charge recombination [16,18].

Measurements of PL decay kinetics enabled one to determine the lifetime of non-equilibrium charge carriers equal to 25 ns (Figure 2b).

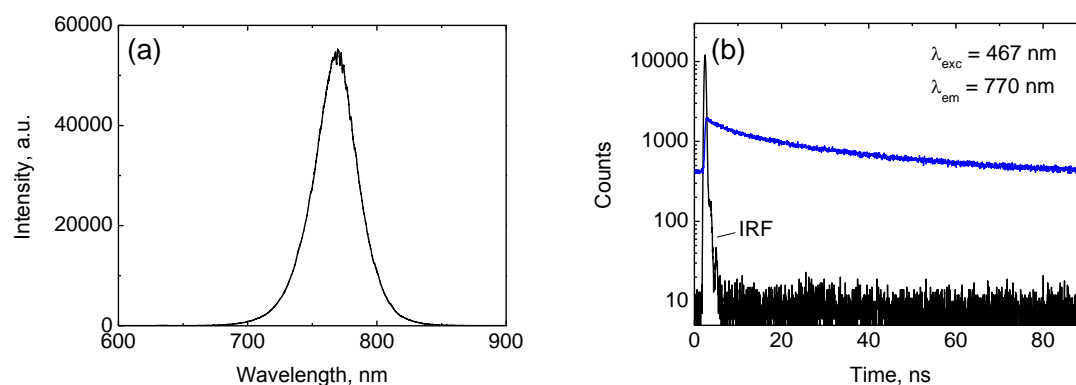


Figure 2. Room temperature PL spectrum (a) and decay kinetics (b) for $\text{CH}_3\text{NH}_3\text{PbI}_3$ film.

It is a matter of common knowledge that the intensity of interband radiative recombination decreases with increasing imperfection degree of material due to the increased probability of competing non-radiative recombination channel. Spectral position of PL maximum is determined by the electron density of states (DOS). In particular, the presence of pronounced tails of DOS (a large Urbach energy) leads to a red shift of PL maximum, which was observed for perovskites by many authors [19,20]. Hence, analysis of PL intensity and peak position enables one to track variation of perovskite film quality under influence of different impacts. Available literature data regarding Raman spectroscopy of $\text{CH}_3\text{NH}_3\text{PbI}_3$ are rather contradictory, and there are some discrepancies between the theoretical and experimental data [18]. Nevertheless, Raman spectroscopy makes it possible to detect PbI_2 as the degradation product of $\text{CH}_3\text{NH}_3\text{PbI}_3$ layers.

In our experiments, optical exposure of the films was carried out in the following sequence. It is known that illumination of the $\text{CH}_3\text{NH}_3\text{PbI}_3$ films can give rise to increase in intensity of their photoluminescence, which is usually related to change in the charge state of defects acting as centers of non-radiative recombination [21]. Therefore, the films were subjected to light soaking using a low-intensity illumination prior to study of influence of high-power light exposure on their properties. For this purpose, fifty PL spectra were measured sequentially with the focusing of the laser beam at the same point on the film surface. The signal acquisition time in each measurement was 5 s at the optical power of $0.6 \mu\text{W}$. The experiments have shown that such exposure leads to a gradual two-fold increase in PL intensity with subsequent attainment of saturation. Then the film was subjected to a high-intensity optical exposure for 30 s, and PL spectrum was measured again. The power of each subsequent optical exposure was increased, whereas the mode of PL spectrum measurement after each exposure was the same (signal acquisition time of 5 s and optical power of $0.6 \mu\text{W}$). Maximum optical power used was $600 \mu\text{W}$.

Figure 3a presents PL maximum position and intensity for the $\text{CH}_3\text{NH}_3\text{PbI}_3$ film depending on the power of preceding optical exposure. As is seen, dependence of peak position is characterized by a pronounced minimum. It means that exposure of the films with a relative low power does not deteriorate, but even improves the quality of the material. At the same time, exposure with a greater power makes material more defective, which correlates with the decrease in the PL signal intensity and appearance of the bands corresponding to PbI_2 in the Raman spectra (Figure 3b).

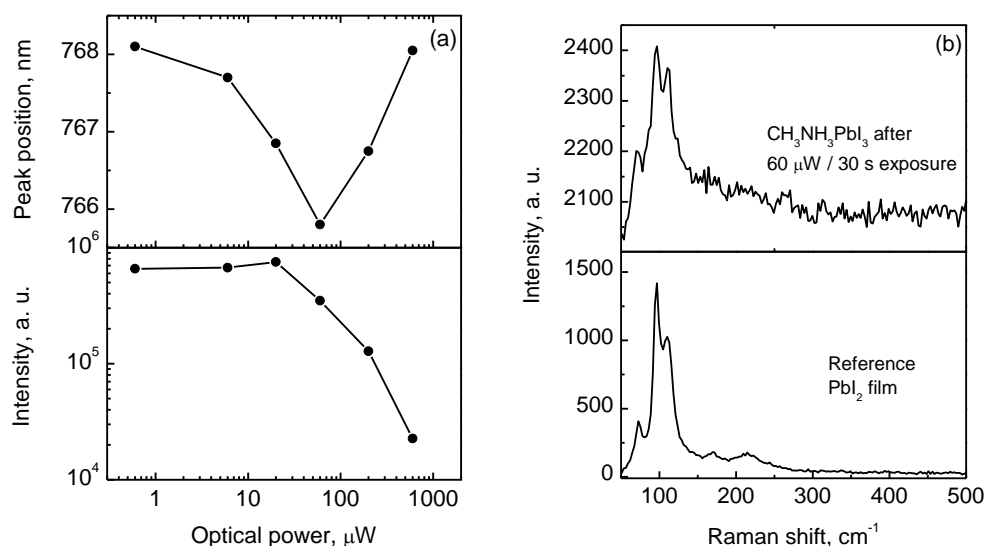


Figure 3. (a): PL maximum position and intensity for the $\text{CH}_3\text{NH}_3\text{PbI}_3$ film depending on power of preceding optical exposure; lines are given for convenience; (b): Raman spectra of $\text{CH}_3\text{NH}_3\text{PbI}_3$ film subjected to $60 \mu\text{W}$ / 30 s optical exposure and reference PbI_2 film.

There are different hypotheses regarding mechanisms of light soaking induced improvement of properties of $\text{CH}_3\text{NH}_3\text{PbI}_3$ films. In particular, it was reported that illumination can result in a reversible structural transformation of $\text{CH}_3\text{NH}_3\text{PbI}_3$ lattice [22]. However, taking into account high densities of optical power in our experiments, one can suppose that the observed effect is related rather to optical annealing of the film.

Knowing the diameter of the light spot on the sample surface during measurement of PL spectra ($\approx 0.8 \mu\text{m}$), one can estimate the ranges of optical power density corresponding to the observed changes in film properties. So, the quality of the $\text{CH}_3\text{NH}_3\text{PbI}_3$ film deteriorates only when power density exceeds 10^8 W/m^2 , whereas the optical impact on the films with power density less than $4 \cdot 10^7 \text{ W/m}^2$ improves their quality.

4. Conclusion

$\text{CH}_3\text{NH}_3\text{PbI}_3$ films were characterized with different spectroscopic techniques. It was revealed that exposure of the $\text{CH}_3\text{NH}_3\text{PbI}_3$ films with a monochromatic light ($\lambda = 532 \text{ nm}$) with intensity less than $4 \cdot 10^7 \text{ W/m}^2$ results in a blue shift of interband photoluminescence, which is related to decrease in the Urbach energy and points to improvement of film perfection. At the same time, film exposure at a power density more than 10^8 W/m^2 leads to decrease in intensity of PL band, its red shift and appearance in the Raman spectra of bands corresponding to PbI_2 phase. Thus, the ranges of light intensity corresponding to both degradation and improvement of the $\text{CH}_3\text{NH}_3\text{PbI}_3$ films quality are determined.

Acknowledgements

This work was supported by the Russian Science Foundation, grant no. 15-13-00170. O.K., A.M., and M.T. acknowledge financial support by the Belarusian Republican Foundation for Fundamental Research (project F16MS-015).

References

- [1] Kojima A, Teshima K, Shirai Y and Miyasaka T 2009 *Am. Chem. Soc.* **131** pp 6050–6051
- [2] Liu D Y and Kelly L 2014 *Nat. Photonics.* **8** pp 133–138
- [3] Bae S, Park JS, Han IK, Shin TJ and Jo WH 2017 *Solar Energy Materials & Solar Cells.* **160** pp 77–84
- [4] Gladyshev P P, Yushankhai V Y and Syurakshina L A 2015 *Ivan. Gos. University Press.* 676 pp 426-556
- [5] Zhao Y and Zhu K 2016 *Chem. Soc. Rev.* **45** pp 655-689
- [6] Heo J, Im S, Noh J, Mandal T, Lim C, Chang J, Lee Y, Kim H, Sarkar A, Nazeeruddin M, Grätzel M and Seok S 2013 *Nat Photonics.* **7** pp 487–492
- [7] Xiao M, Huang F, Huang W, Dkhissi Y, Zhu Y, Etheridge J, Gray-Weale A, Bach U, Cheng Y-B and Spiccia L 2014 *Angew. Chem., Int. Ed.* **53** pp 9898-9903
- [8] Della Gaspera E, Peng Y, Hou Q, Spiccia L, Bach U, Jasieniak J and Cheng Y 2015 *Energy.* **13.** pp 249-257
- [9] Liang K, Mitzi D. B and Prikas M T *Chem. Mater.* **10** pp 403-411.
- [10] Burschka J, Pellet N, Moon S J, Humphry-Baker R, Gao P, Nazeeruddin M K and Gratzel M 2013 *Nature* **499** pp 316-319
- [11] Im J-H, Kim H-S, Park N-G 2014 *APL Materials.* **2** 081510
- [12] O'Connor D V and Phillips D 1984 *Time-correlated Single Photon Counting N.Y.: Acad. Press* 283 p.
- [13] Chen Q, Zhou H, Hong Z and Luo S 2014 *J. Am. Chem. Soc.* **136** pp 622-625
- [14] Jeon Y-J, Lee S, Kang R, Kim J-E, Yeo J-S, Lee S-H, Kim S-S, Yun J-M and Kim D-Y 2014 *Subject Areas.* **4** 6953-1–6953-8
- [15] Duyen H C et al 2014 *APL Materials.* **2** 091101
- [16] Shi D, Adinolfi V, Comin R, Yuan M and Alarousu E 2015 *Science.* **347** pp 519-522

- [17] Abdelhady A L, Saidaminov M I, Murali B and Adinolfi V 2016 *J. Phys. Chem. Lett.* **7** pp 295–301
- [18] Park B-W, Jain S M, Zhang X, Hagfeldt A, Boschloo G and Edvinsson T 2015 *ACS Nano, ACS Nano.* **9** pp 2088–2101
- [19] Yang D, Yang R, Ren X, Zhu X, Yang Z, Li C and Liu S 2016 *Adv. Mater.* **28** pp 5206–5213
- [20] Shao Y, Xiao Z, Bi C, Yuan Y and Huang J 2014 *Nature Communications* **5** 5784
- [21] Zhao C, Chen B, Qiao X, Luan L, Lu K and Hu B 2015 *Adv. Energy Mater.* **5** 1500279
- [22] Gottesman R, Gouda L, Kalanoor B S, Haltzi E, Tirosh S, Rosh-Hodesh E, Tischler Y and Zaban A 2015 *J. Phys. Chem. Lett.* **6** pp 2332–2338.